





Article

Analysis of Different Third-Generation Solar Cells Using the Discrete Electrical Model d1MxP

João Paulo N. Torres ^{1,2,*} , Ricardo A. Marques Lameirinhas ^{2,3,*} , Catarina Pinho Correia Valério Bernardo ^{2,3} , Sofia Lima Martins ³, Pedro Mendonça dos Santos ^{1,2}, Helena Isabel Veiga ¹ , Maria João Marques Martins ¹ and Paula Manuela Santos do Rego Figueiredo ¹

¹ Academia Militar/CINAMIL, Av. Conde Castro Guimarães, 2720-113 Amadora, Portugal

² Instituto de Telecomunicações, 1049-001 Lisbon, Portugal

³ Department of Electrical and Computer Engineering, Instituto Superior Técnico, 1049-001 Lisbon, Portugal

* Correspondence: joaoptorres@hotmail.com (J.P.N.T.); ricardo.lameirinhas@tecnico.ulisboa.pt (R.A.M.L.)

Abstract: The performance of photovoltaic solar cells is usually analyzed using continuous models, for instance, 1M5P. I-V and P-V curves are fitted by a mathematical expression from the electrical model. In the case of 1M5P, characteristics are fitted using five parameters that are obtained using a small number of I-V points from a wider set of data, keeping the curve shape given by the mathematical expression from the model. A novel model was recently proposed to overcome this issue. The d1MxP model is based on the discretization of the electrical behavior of the diodes in models such as 1M5P. The d1MxP methodology is equivalent to an analytical incremental calculation and since it connects the given points, the model error should be lower than the one obtained using models as 1M5P. It is based on the connection of adjacent points (with small voltage differences) instead of having the entire voltage range represented by some parameters (as the continuous models do, for instance, 1M5P). In this work, the d1MxP model is applied to perovskite solar cells and paint-type dye-sensitized solar cells. The aim is to analyze the behavior of the discrete model in different third-generation solar cells since their performance cannot be well characterized by the 1M5P model. The accuracy on the maximum power point is relevant, resulting in perovskite solar cells, an improvement of up to 2.61% and, in paint-type dye-sensitized solar cells, an increase of up to 5.03%.

Keywords: 1M5P; d1MxP; perovskite solar cells; paint-type dye-sensitized solar cell; photovoltaic technology; solar cell equivalent model; solar energy



Citation: Torres, J.P.N.; Marques Lameirinhas, R.A.; Pinho Correia Valério Bernardo, C.; Lima Martins, S.; Mendonça dos Santos, P.; Veiga, H.I.; Marques Martins, M.J.; Santos do Rego Figueiredo, P.M. Analysis of Different Third-Generation Solar Cells Using the Discrete Electrical Model d1MxP. *Energies* **2023**, *16*, 3289. <https://doi.org/10.3390/en16073289>

Academic Editors: Alessandro Ciocia and Antonio D'Angola

Received: 18 March 2023

Revised: 29 March 2023

Accepted: 1 April 2023

Published: 6 April 2023



Copyright: © 2023 by the authors. Licensee MDPI, Basel, Switzerland. This article is an open access article distributed under the terms and conditions of the Creative Commons Attribution (CC BY) license (<https://creativecommons.org/licenses/by/4.0/>).

1. Introduction

Since the Industrial Revolution, the need for energy production has increased considerably. This revolution involved a transition to new manufacturing processes, such as the replacement of hand production methods with machines that used fossil fuels in their operation. Additionally, the replacement of firewood (which was until then the main energy source) with coal was also significant. Therefore, the use of coal in steam engines was paramount to the industrial development of humankind. However, the use of fossil fuels and non-renewable energy sources has a negative impact on the environment, resulting in an increase in average global temperatures and the greenhouse effect. Furthermore, they are a limited energy source. Over the years, concerns about the environment have significantly increased due to the current climate crisis that the world is facing.

Thus, in the last decades, the focus on renewable sources for energy production has been growing, especially solar energy, which has reached installation record values, due to its relatively low production cost and ease of installation [1–5].

In the 19th century, the photovoltaic effect was discovered by a French physicist. Since then, the development of solar cells has evolved into different generations. The first generation is mainly composed of silicon solar cells and single junctions. The second consists

of thin film technologies, and the third and latest generation is composed of organic solar cells, such as perovskite and dye-sensitized [1,6]. Both types of solar cells have been considered as a new paradigm for solar cells, with reduced costs and increased efficiency [7–9]. However, both technologies face certain challenges regarding their limitations.

In 2009, the prototype of a perovskite photovoltaic solar cell was demonstrated with 3.8% efficiency. Over the following years, their power conversion rapidly increased to more than 20% [1,10–13]. These solar cells have several factors that contribute to their low lifetime, meaning their module viability is not high. This can be explained by the origin of the compounds used, such as spiro-OMeTAD, which has a solvent origin, leading to devices that are more sensitive to oxidation and humidity [12]. Thus, their behavior can be more unstable [1,14], and as a result, there is still a long way to go until viable mass manufacturing of perovskite solar cells can be achieved due to these reproducibility issues. In 1991, dye-sensitized solar cells, also known as Grätzel cells, were verified with an efficiency of 7%; in 1997, an efficiency of 10% was registered at the National Renewable Energy Laboratory (NREL) [9,15]. In recent years, some of the limitations associated with these cells have been evaluated, which can be divided into extrinsic and intrinsic stability. Concerning intrinsic stability, aging experiments were performed as reported in reference [15], and it was concluded that rapid degradation occurs with light soaking and temperatures of about 80 °C, which can be easily attained during sunny days.

The performances of these devices vary with external conditions, such as temperature and irradiance. The cell's maximum power point is highly influenced by the cell's temperature and, therefore, its efficiency. Consequently, it has a huge impact on the behavior of the characteristic curves. In reference [16], the authors studied the temperature impact on perovskite solar cells under operation and found that at low temperatures, the devices present very stable values, with an average loss lower than 5%. However, at high temperatures, experimentally verified decreases in the open-circuit potential and the short-circuit current are observed.

To describe the behavior of these devices, electrical models can be used, such as 1M3P, which is an electrical model composed of three parameters; it does not take into account internal circuit losses, 1M5P and 1M7P, which are electrical models with five and seven parameters, respectively [1,17–21]. All of these models have as their first goal the characterization of the behavior of the devices with the highest possible accuracy [1,17,22]. However, when the cell or a set of cells are under extreme conditions, such as high temperatures, partial shading, and cracks, these models do not have the best accuracy and, as a result, cannot represent the correct behavior of these devices. In reference [2], an example of this is given. Under the "cracks" situation, I-V experimental points were fitted using a mathematical model of a double exponential model, which, in practice, consists of a parallel connection of two photodiodes. This example shows that these models have limitations when the devices are not under standard conditions.

To resolve this, a new method was created in order to characterize solar cells with higher accuracy, under extreme and non-extreme conditions. The novel d1MxP model is a discrete electrical model with x parameters; its methodology is presented in the next section. This model is based on the graphical connection between consecutive I-V points [17]. The novel d1MxP is based on the discretization and linearization of the diode's electrical behavior and the physical phenomena in a p-n junction. This is accomplished by using electrical branches with an ideal diode, a voltage source, and resistance, with their values serving as the model's fitting parameters.

The aim of this work is to analyze the behavior of this novel model in different third-generation solar cells. In this study, we analyzed perovskite and dye-sensitized solar cells. Moreover, we analyzed this model in a unique dye-sensitized solar cell, i.e., a paint-type.

These types of solar cells are known to have electrical behaviors that are different from silicon solar cells (simple p-n junctions). Thus, the I-V characteristic of a regular 1M5P model does not fit well on the performance. The novel d1MxP model allows for connecting adjacent points and, consequently, it might bring some advantages to characterize these

types of solar cells. It has been suggested that more complex structures, such as the ones analyzed in this work, and others, such as tandem or metalized solar cells, might be better modeled using the d1MxP model, as it connects experimental points instead of fitting a certain shape. The goal of this work is to investigate and compare the results of both models and conclude on the possibility of using d1MxP.

2. Methodology

The explanation and deduction of the model are better explained in reference [17], where the model is introduced and validated. It is based on connecting adjacent points with small voltage differences, instead of having parameters to fit the entire voltage range, as continuous models do, e.g., 1M5P.

The discretization was done using the diode’s equivalent circuit/model, consisting of an ideal diode, resistance, and an independent voltage source in series. A branch with an ideal diode, resistance, and a voltage source is used to connect two I-V points. The electrical model is presented in Figure 1 for N+1 points (N branches and N connections).

The diode in 1M5P is replaced by N branches, and the electrical behaviors of the resistances in 1M5P are within these N branches. This means that the electrical behavior of the photovoltaic solar cell is linearized at each I-V point.

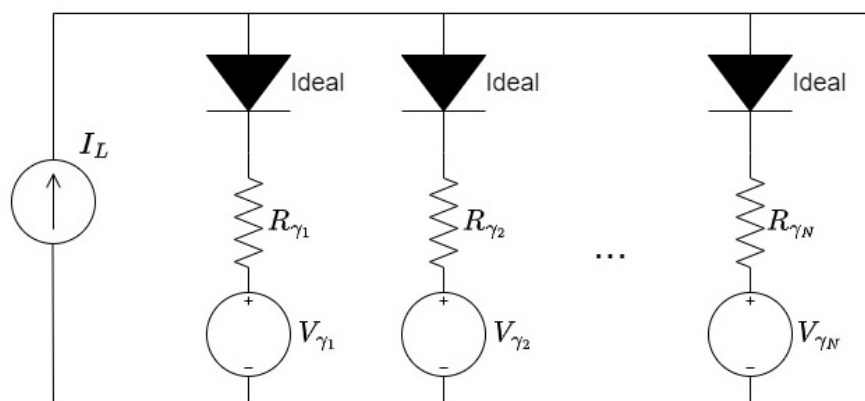


Figure 1. Proposed equivalent circuit model of a photovoltaic solar cell: d1MxP.

An example of the obtained I-V curves using this discretization is presented in Figure 2, where the electrical behavior of the photovoltaic solar cell is linearized using four branches (eight parameters). The exponential shape of the solar cell might be obtained using a finite number of branches, meaning that one might adjust the curve shape even if it is not exponential.

Equation set 1 is used to obtain the model parameters. The deduction and explanation are presented in reference [17] and are based on the fact that the ideal diode will be activated at voltages higher than V_{γ} , leading to a slope proportional to R_{γ} . However, all of the activated branches have an influence on the I-V slope, meaning that the resistance of branch N+1 is not proportional to the slope of that connection, but rather to the inclination (slope variation). In other words, the slope of the I-V curve is related to all of the activated resistances, which are in parallel. On the other hand, the V_{γ} values are obtained from experimental data.

$$\begin{cases} V_{\gamma} = V_i \\ R_{\gamma} = -\frac{1 + m_i m_{i-1}}{m_i - m_{i-1}} \end{cases} \tag{1}$$

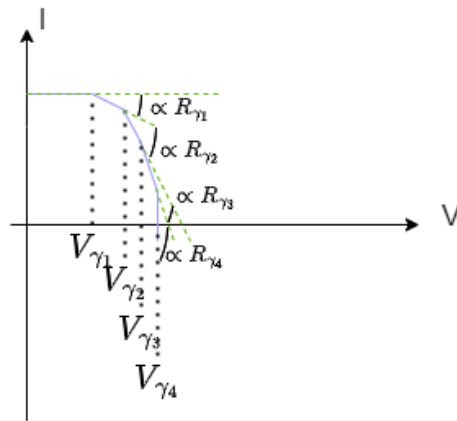


Figure 2. An example of an I-V characteristic based on the d1MxP model with 4 branches ($N = 4$).

The results from d1MxP are also compared with the 1M5P ones. The I-V function of the classical model is determined by expression (2), where I_L , I_d , and I_{sh} represent the photogenerated current, the current that passes through the diode, and the current that passes through the shunt resistance R_{sh} (associated with the current loss due to current leaks on the cell), respectively. The current I_d depends on the diode reverse current, I_o , the diode non-ideality factor n , the series resistance R_s (associated with the voltage loss due to the cell connections), and the thermal voltage V_T , given by expression (3), where k is the Boltzmann’s constant, T is the temperature, and q is the electron charge. However, in this model, the current depends on itself. For that reason, the Newton–Raphson method is applied as presented in expression (4), where $f(I)$ corresponds to expression (2) and $f'(I)$ is its first derivative, with respect to I . For each I-V point, the current value is iterated, with i being the iteration index.

$$I = I_L - I_d - I_{sh} = I_L - I_o \left(e^{\frac{V+R_s I}{nV_T}} - 1 \right) - \frac{V + R_s I}{R_{sh}} \tag{2}$$

$$V_T = \frac{kT}{q} \tag{3}$$

$$I_{i+1} = I_i - \frac{f(I)}{f'(I)}. \tag{4}$$

Before using expression (2), the five parameters of 1M5P should be obtained, based on expressions (5) and (6) [1,17,18].

$$\begin{cases} R_s = -\frac{1}{\frac{dI}{dV}|_{V=V_{OC}}} \\ R_{sh} = -\frac{1}{\frac{dI}{dV}|_{I=I_{SC}}} \\ I_o = \frac{I_{SC} \left(1 + \frac{R_s}{R_{sh}} \right) - \frac{V_{OC}}{R_{sh}}}{e^{\frac{V_{OC}}{nV_T}}} \\ I_L = I_o \left(e^{\frac{V_{OC}}{nV_T}} - 1 \right) + \frac{V_{OC}}{R_{sh}} \end{cases} \tag{5}$$

$$\begin{aligned} n \rightarrow \ln \left(I_{SC} \left(1 + \frac{R_s}{R_{sh}} \right) - \frac{V_{mp}}{R_{sh}} - I_{mp} \left(1 + \frac{R_s}{R_{sh}} \right) \right) = \\ \ln \left(I_{SC} \left(1 + \frac{R_s}{R_{sh}} \right) - \frac{V_{OC}}{R_{sh}} \right) - \frac{V_{OC}}{nV_T} + \frac{V_{mp} + R_s I_{mp}}{nV_T}. \end{aligned} \tag{6}$$

The main disadvantage of models such as 1M5P is that the entire voltage range is characterized by the same mathematical expression, which is prone to local inaccuracies and, consequently, results in worse fittings. This becomes more relevant in obtaining the maximum power, efficiency, fill factor, and other important figures of merit.

The complexity of determining the 1M5P parameters is high. Moreover, sometimes the application of these expressions gives non-real results, even with an excellent experimental dataset. Moreover, 1M5P only has five parameters, and it already has that disadvantage. With more parameters, for instance, seven, the complexity is even higher, and the deduction of final expressions to be applied to the model is not simple, leading to the application of some very restrictive equations.

The d1MxP methodology is equivalent to an analytical incremental calculation; since it connects the given points, the model error should be lower than the one obtained using models such as 1M5P.

3. Results

3.1. Perovskite Solar Cells

In order to evaluate the behavior of the discrete model in perovskite solar cells, two different devices were tested. The experimental data used are obtained from the literature [16].

Figure 3 presents the experimental data of a representative device with spiro-OMeTAD as HEL, with an area of 1 cm², operating at a room temperature of 22 °C. The I-V curve resulting from the 1M5P and the one resulting from the d1MxP are shown in yellow and red, respectively. Based on Equations (5) and (6), it is possible to obtain the parameters that characterize the 1M5P. They are $I_L = 0.0172$ A, $I_o = 9.7636 \times 10^{-12}$ A, $n = 1.9181$, $R_{sh} = 7924.5283$ Ω, and $R_s = 4.1465$ Ω. Table 1 presents the parameter values for each branch of the d1MxP. Using the experimental points, the model has 20 branches, and each branch is characterized by two parameters. In this case, the discrete model can be called d1M40P. As can be seen, the novel discrete model results in more accurate fittings in the voltage range when compared to the 1M5P results. Furthermore, it can be verified through Table 1 and Figure 3 that the higher the slope variation in the I-V curve, the lower the resistance value in the model's branch. This discrete model does not have, in its equivalent electrical circuit, the two resistances that characterize the system's losses in the classical model, 1M5P. However, the resistance of the first branch of the discrete model corresponds to the shunt resistance, associated with current losses, due to the fact that this first resistance is associated with a null voltage. It can be verified through the first line of Table 1 and the shunt resistance value of the 1M5P. Since the discrete model tracks the experimental data well, the series resistance associated with voltage losses (which is not computed in this model) is taken into account through the slope variation near the open circuit. The behavior of the 1M5P series resistance has no direct correspondence, but it is treated on the resistances near the open-circuit point.

The P-V characteristic curves at 22 °C are presented in Figure 4 for the d1MxP model and the one obtained with the 1M5P model. The discrete model, represented in red, fits better with the I-V data, leading to a more accurate determination of the maximum power point.

Figure 5 shows the I-V characteristic curves of a different perovskite solar cell, with an area of 1 cm², operating at the same temperature as the previous one. For the device prepared with pristine spiro-OMeTAD, the 5 parameters of the 1M5P are $I_L = 0.0179$ A, $I_o = 3.8157 \times 10^{-13}$ A, $n = 1.4631$, $R_{sh} = 4.1176 \times 10^{11}$ Ω, and $R_s = 7.5404$ Ω. These parameters are obtained by Equations (5) and (6). Using the discrete model, the computed parameters are presented in Table 2. At this temperature, this device can be represented through 14 branches, being x equal to 28, which is the number of parameters (d1M28P). Once again, as in the previous case, the shunt resistance value corresponds to the resistance value of the first branch ($N = 1$) of the discrete model. Through Figure 5, it is more clear

that d1MxP presents more accuracy, significantly reducing the error obtained from the 1M5P model.

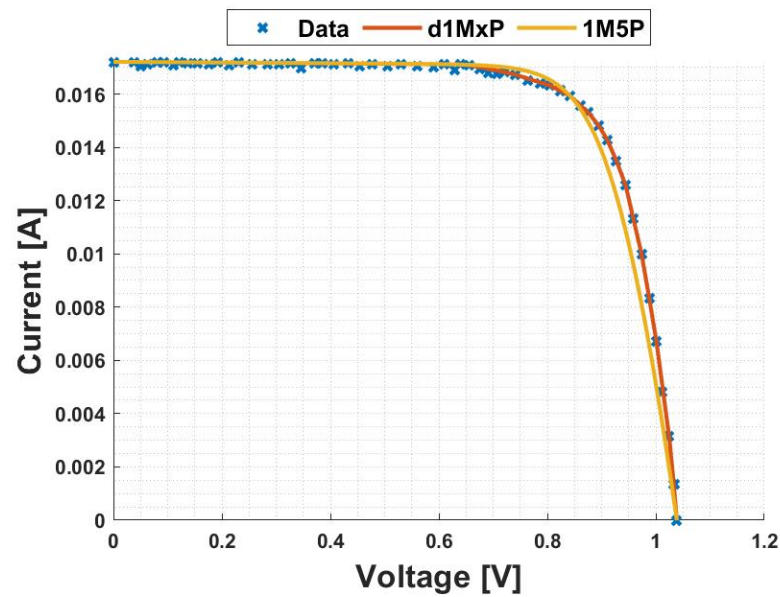


Figure 3. Spiro-OMeTAD as HEL I-V curves at $T = 22\text{ }^{\circ}\text{C}$, from 1M5P and d1MxP models.

Table 1. Parameters of d1MxP applied on spiro-OMeTAD as HEL for $T = 22\text{ }^{\circ}\text{C}$.

| N | $R_{\gamma} [\Omega]$ | $V_{\gamma} [V]$ |
|-----|-----------------------|------------------|
| 1 | 7924.5283 | 0 |
| 2 | 125,003.0453 | 0.0377 |
| 3 | 46,155.2119 | 0.1915 |
| 4 | 583.5560 | 0.6396 |
| 5 | 478.6033 | 0.6566 |
| 6 | 1178.7960 | 0.7208 |
| 7 | 615.0313 | 0.7406 |
| 8 | 273.0927 | 0.8047 |
| 9 | 1882.2774 | 0.8236 |
| 10 | 123.9662 | 0.8415 |
| 11 | 152.9023 | 0.8755 |
| 12 | 118.9689 | 0.8943 |
| 13 | 76.5353 | 0.9104 |
| 14 | 134.0653 | 0.9274 |
| 15 | 29.8052 | 0.9443 |
| 16 | 35.1641 | 0.9736 |
| 17 | 171.0759 | 0.9877 |
| 18 | 34.5110 | 1.0009 |
| 19 | 18.0137 | 1.0245 |
| 20 | 33.0539 | 1.0330 |

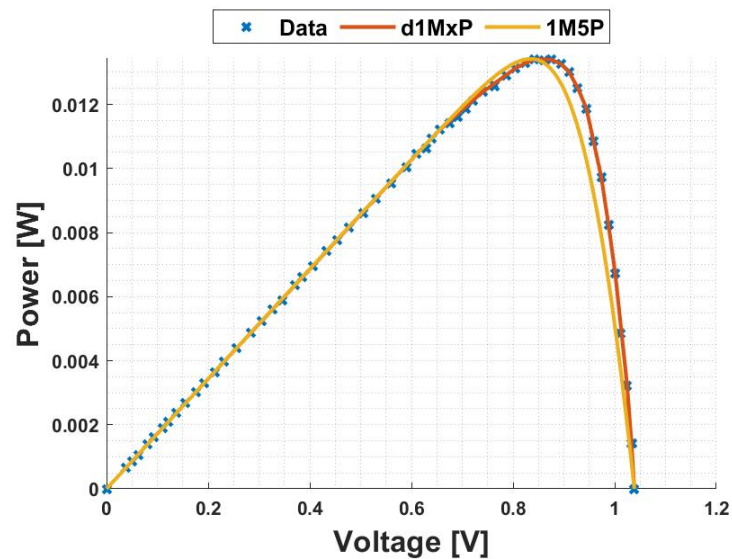


Figure 4. Spiro-OMeTAD as HEL P-V curves at $T = 22\text{ }^{\circ}\text{C}$, from 1M5P and d1MxP models.

The P-V characteristic curves are presented in Figure 6. In this situation, as expected, d1MxP fits the experimental data more accurately when compared with 1M5P. This has a huge impact on the maximum power point.

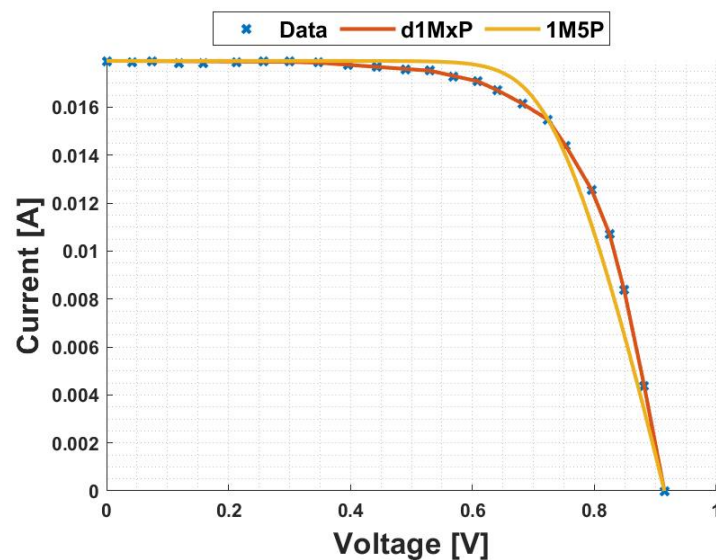
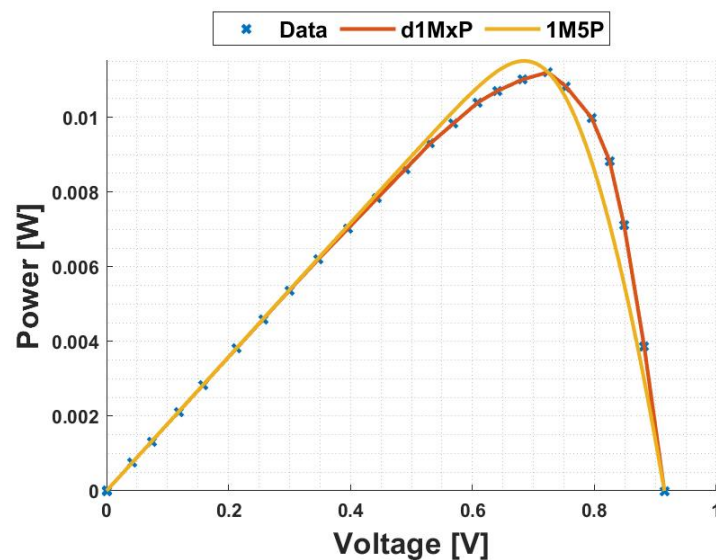


Figure 5. Pristine spiro-OMeTAD I-V curves at $T = 22\text{ }^{\circ}\text{C}$, from 1M5P and d1MxP models.

Table 3 presents an important summary to compare the maximum power points (power, voltage, and current) for the two different perovskite solar cells. The differences between the proposed d1MxP and the 1M5P models are also determined and presented, taking the 1M5P results as a reference. There are significant differences between both models, with the discrete model allowing a correction of the values of about 0.07% to 2.61% in the maximum power, 0.87% to 5.70% in the maximum voltage value, and 0.87% to 7.86% in the maximum current.

Table 2. Parameters of d1MxP applied on pristine spiro-OMeTAD for T = 22 °C.

| N | R_γ [Ω] | V_γ [V] |
|----|-------------------------|-----------------------|
| 1 | 4.1176×10^{11} | 0 |
| 2 | 8099.7302 | 1.00×10^{-5} |
| 3 | 1532.4422 | 0.3000 |
| 4 | 956.0864 | 0.3477 |
| 5 | 259.9907 | 0.5307 |
| 6 | 167.4610 | 0.6091 |
| 7 | 515.5360 | 0.6409 |
| 8 | 439.5374 | 0.6818 |
| 9 | 46.0024 | 0.7239 |
| 10 | 180.2672 | 0.7534 |
| 11 | 51.3815 | 0.7955 |
| 12 | 28.6649 | 0.8250 |
| 13 | 42.8730 | 0.8489 |
| 14 | 90.4095 | 0.8818 |

**Figure 6.** Pristine spiro-OMeTAD P-V curves at T = 22 °C, from 1M5P and d1MxP models.**Table 3.** Maximum power (P_{max}), maximum voltage (V_{max}), and maximum current (I_{max}) values from both models.

| | | d1MxP | 1M5P | Δ (%) |
|-----------------------|---------------|---------|---------|--------------|
| Spiro-OMeTAD as HEL | P_{max} [W] | 0.01341 | 0.01342 | 0.07 |
| | V_{max} [V] | 0.84151 | 0.83427 | 0.87 |
| | I_{max} [A] | 0.01594 | 0.01608 | 0.87 |
| Pristine spiro-OMeTAD | P_{max} [W] | 0.01121 | 0.01151 | 2.61 |
| | V_{max} [V] | 0.72386 | 0.68485 | 5.70 |
| | I_{max} [A] | 0.01548 | 0.01680 | 7.86 |

3.2. Dye-Sensitized Solar Cell

In the literature, a paint-type dye-sensitized solar cell has been reported [23]. This type of solar cell is based on two electrodes, and the substrates were painted using two kinds of paint. The paint material used in this study was carbon nanotubes, which are known to have a range of useful properties. In fact, these nanostructures have both semiconducting and

metallic properties, which can be advantageous for increasing the efficiency of the device. The emergence of these types of solar cells has opened up new applications, particularly those that were previously not possible due to installation issues. The experimental I-V points for this type of solar cell were obtained from [23], and the novel discrete model was tested on this device to analyze the advantages of using the discrete model.

Figures 7 and 8 show the I-V and P-V characteristics of the experimental data of a paint-type dye-sensitized solar cell. Moreover, both figures present the characteristic curves resulting from the 1M5P (represented in yellow) and the one resulting from the discrete model (represented in red). The classical 1M5P model has the following five parameters: $I_L = 0.0004$ A, $I_o = 3.0107 \times 10^{-13}$ A, $n = 0.6076$, $R_{sh} = 6523.2558 \Omega$, and $R_s = 444.7674 \Omega$. All of these parameters are, once again, calculated through Equations (5) and (6). Regarding the d1MxP, Table 4 summarizes the discrete model parameters for each branch. Using the experimental data, the model has 19 branches and 38 parameters (d1M38P). By comparing the shunt resistance value of the 1M5P with the resistance value of the first branch of the discrete model, it is possible to corroborate the statement that the resistance of the first branch corresponds to the resistance that takes into account the current losses of the 1M5P. The I-V curve obtained using the d1MxP model shows excellent agreement with the experimental data, with the 1M5P model results used as a reference. However, using the classic model can result in higher errors, especially in the maximum power point. This can be seen in the P-V curve presented in Figure 8.

Table 5 summarizes the comparison of maximum power points (power, voltage, and current) of a paint-type dye-sensitized solar cell. Considering the 1M5P results as a reference, the difference between the proposed model and the 1M5P model is also observed in the table. In this case, the novel model allows a correction of the values of about 5.03% in the maximum power, 17.17% in the maximum voltage value, and 18.95% in its maximum current.

Regarding the fill factor, the literature reported a value of 40% [23] but with the d1MxP model, the fill factor is increased to 66.91%. This value is computed by calculating the trapezoidal area under the points. This demonstrates an advantage of the d1MxP model, which is more accurate in fitting the experimental points.

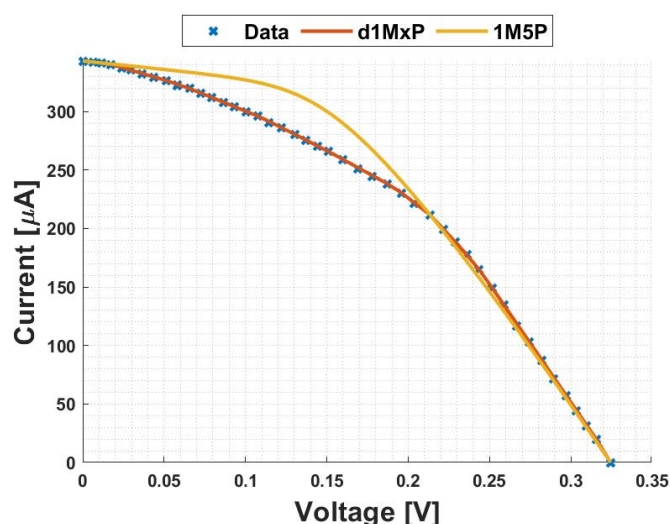


Figure 7. Paint-type dye-sensitized solar cell I-V curves from 1M5P and d1MxP models.

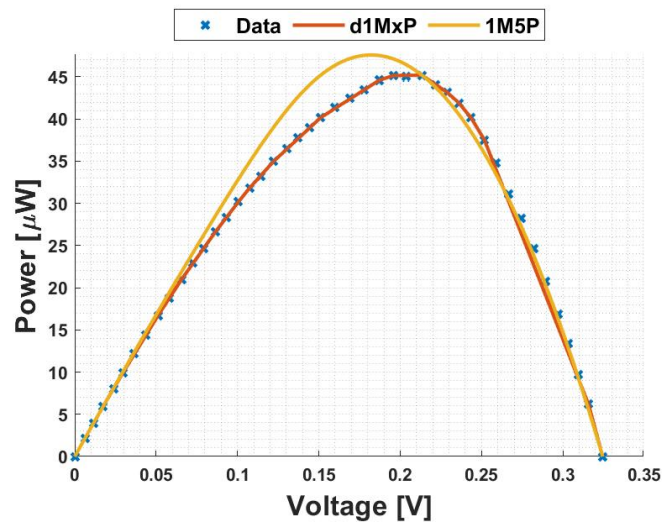


Figure 8. Paint-type dye-sensitized solar cell P-V curves from 1M5P and d1MxP models.

Table 4. Parameters of d1MxP applied on the paint-type dye-sensitized solar cell.

| N | R_{γ} [Ω] | V_{γ} [V] |
|-----|---------------------------|------------------|
| 1 | 6523.2558 | 0 |
| 2 | 41,313.9546 | 0.0064 |
| 3 | 4464.4584 | 0.0174 |
| 4 | 115,194.7864 | 0.0297 |
| 5 | 16,133.7241 | 0.0512 |
| 6 | 11,119.1890 | 0.0657 |
| 7 | 3.6893×10^{17} | 0.0866 |
| 8 | 1.5372×10^{18} | 0.1006 |
| 9 | 8895.3522 | 0.1076 |
| 10 | 29,651.1770 | 0.1221 |
| 11 | 18,758.9090 | 0.1512 |
| 12 | 7256.7369 | 0.1872 |
| 13 | 5930.2383 | 0.1959 |
| 14 | 2320.5295 | 0.2134 |
| 15 | 21,348.8867 | 0.2291 |
| 16 | 7116.2976 | 0.2360 |
| 17 | 4151.1763 | 0.2436 |
| 18 | 10,377.9474 | 0.2517 |
| 19 | 4447.6947 | 0.3157 |

Table 5. Maximum power (P_{max}), maximum voltage (V_{max}), and maximum current (I_{max}) from both models.

| | d1MxP | 1M5P | Δ (%) |
|----------------------|-----------|-----------|--------------|
| P_{max} [μ W] | 45.18468 | 47.57921 | 5.03 |
| V_{max} [V] | 0.21337 | 0.18210 | 17.17 |
| I_{max} [μ A] | 211.76470 | 261.27779 | 18.95 |

4. Conclusions

The aim of this work was to analyze the novel discrete model in different third-generation solar cells. Although the behaviors of these devices can be described using classic models, they do not provide accurate analyses of the experimental data. The I-V characteristics of a regular 1M5P model do not fit well with the performance of these devices. The novel d1MxP model allows for the connection of adjacent points, providing some advantages in characterizing these types of solar cells. The d1MxP is based on the discretization and linearization of the diode's electrical behavior. The goal of this work is to investigate and compare the results of both models and conclude on the possibility of using the d1MxP.

The presented results show that the novel discrete d1MxP model is a good solution to characterize the behaviors of different and complex solar cells. Regarding the paint-type dye-sensitized solar cell, its I-V curve does not have the typical form of a solar cell's I-V curve, which is a challenge for the novel approach.

With the various third-generation solar cells under analysis, it can be seen that the mathematical and electrical d1MxP model allows for the computation of more accurate I-V and P-V curves, fitting the experimental I-V points better. This is due to the fact that the discrete model uses a larger portion of experimental points to describe the devices compared to the classical models presented in the literature that use a small portion of the data set to characterize the entire voltage range. The significant difference is observed at the maximum power point, resulting in an increase in the fill factors of these devices, and allowing to obtain more accurate figures of merit, such as efficiency. It was also noted that, for the solar cells studied, the higher the slope variation, the lower the resistance value.

In perovskite solar cells, improvements of up to 2.61% in the maximum power, 5.70% in voltage, and 7.86% in current were seen. Regarding the paint-type dye-sensitized solar cell, increases of 5.03%, 17.17%, and 18.95% in the maximum power, voltage, and current, were observed, respectively. Furthermore, the fill factor value increased to 66.91%. The results demonstrate that the discrete model is particularly effective for curves with atypical behavior, allowing for a more accurate fit of essential figures of merit in solar cell analysis. Improvements in the estimation of these figures of merit can lead to better characterization of photovoltaic solar cells and reduced errors when sizing large photovoltaic parks, farms, or power plants.

The discrete model still has some challenges ahead; however, there is no doubt that this model is indeed the one that presents higher accuracy. Until now, electrical models did not consider the possibility of non-linearities in characteristic curves. The d1MxP, by considering all experimental points and optimizing, solves this main issue. The current global climate and increasing use of solar energy mean that new solar technologies can be developed with different materials and complex structures, exhibiting atypical behavior that requires rigorous mathematical and electrical analysis.

This model is a unique approach that will be increasingly useful in the near future in the analysis of many photovoltaic solar technologies, for instance in real-time analyses and under extreme conditions. It does not fit a certain shape to the experimental data, but instead uses the points to create the curve (shape). Although the number of parameters is higher than in common models, the mathematical formulation to compute them is simpler, leading to a less complex model.

Author Contributions: Conceptualization: J.P.N.T., R.A.M.L., and C.P.C.V.B.; methodology: R.A.M.L. and C.P.C.V.B.; software: R.A.M.L. and C.P.C.V.B.; investigation: J.P.N.T., R.A.M.L., C.P.C.V.B., S.L.M., P.M.d.S., H.I.V., M.J.M.M., and P.M.S.d.R.F.; writing—original draft: R.A.M.L. and C.P.C.V.B. All authors have read and agreed to the published version of the manuscript.

Funding: This research received no external funding.

Institutional Review Board Statement: Not applicable.

Informed Consent Statement: Not applicable.

Data Availability Statement: Not applicable.

Acknowledgments: This work was supported in part by the FCT/MCTES through national funds, EU funds (project UIDB/50008/2020), and by the FCT (research grant UI/BD/151091/2021). Moreover, the authors would like to acknowledge the support of Academia Militar (AM) and Centro de Investigação, Desenvolvimento e Inovação da Academia Militar (CINAMIL) under project GREEN-FAMIL.

Conflicts of Interest: The authors declare no conflict of interest.

References

1. Marques Lameirinhas, R.A.; Torres, J.P.N.; de Melo Cunha, J.P. A Photovoltaic Technology Review: History, Fundamentals and Applications. *Energies* **2022**, *15*, 1823. [[CrossRef](#)]
2. dos Santos, S.A.A.; Torres, J.P.N.; Fernandes, C.A.; Lameirinhas, R.A.M. The impact of aging of solar cells on the performance of photovoltaic panels. *Energy Convers. Manag. X* **2021**, *10*, 100082. [[CrossRef](#)]
3. Pinho Correia Valério Bernardo, C.; Marques Lameirinhas, R.A.; Neto Torres, J.P.; Baptista, A. Comparative analysis between traditional and emerging technologies: economic and viability evaluation in a real case scenario. *Mater. Renew. Sustain. Energy* **2023**, *12*, 1–12. [[CrossRef](#)]
4. Pinho Correia Valério Bernardo, C.; Marques Lameirinhas, R.A.; Neto Torres, J.P.; Baptista, A. The Shading Influence on the Economic Viability of a Real Photovoltaic System Project. *Energies* **2023**, *16*, 2672. [[CrossRef](#)]
5. Chaar, L.E.; lamont, L.A.; El Zein, N. Review of photovoltaic technologies. *Renew. Sustain. Energy Rev.* **2011**, *15*, 2165–2175. [[CrossRef](#)]
6. Asdrubali, F.; Desideri, U. Chapter 7—High Efficiency Plants and Building Integrated Renewable Energy Systems. In *Handbook of Energy Efficiency in Buildings*; Elsevier: Amsterdam, The Netherlands, 2019. [[CrossRef](#)]
7. Green, M.; Ho-Baillie, A.; Snaith, H. The emergence of perovskite solar cells. *Nat. Photon* **2014**, *8*, 506–514. [[CrossRef](#)]
8. Ananthakumar, S.; Kumar, J.R.; Babu, S.M. Third-generation solar cells: concept, materials and performance-an overview. *Emerg. Nanostruct. Mater. Energy Environ. Sci.* **2019**, *23*, 305–339.
9. Wei, D. Dye Sensitized Solar Cells. *Int. J. Mol. Sci.* **2010**, *11*, 1103–1113. [[CrossRef](#)]
10. Futscher, M.H.; Ehrler, B. Efficiency Limit of Perovskite/Si Tandem Solar Cells. *ACS Energy Lett.* **2016**, *1*, 863–868. [[CrossRef](#)]
11. Wang, D.; Wright, M.; Elumalai, N.K.; Uddin, A. Stability of perovskite solar cells. *Sol. Energy Mater. Sol. Cells* **2016**, *147*, 255–275. [[CrossRef](#)]
12. Rong, Y.; Hu, Y.; Mei, A.; Tan, H.; Saidaminov, M.I.; Seok, S.I.; McGehee, M.D.; Sargent, E.H.; Han, H. Sargent and Hongwei Han. Challenges for commercializing perovskite solar cells. *Science* **2018**, *361*. [[CrossRef](#)] [[PubMed](#)]
13. Jacak, J.E.; Jacak, W.A. Routes for Metallization of Perovskite Solar Cells. *Materials* **2022**, *15*, 2254. [[CrossRef](#)] [[PubMed](#)]
14. Ndione, P.F.; Yin, W.J.; Zhu, K.; Wei, S.H.; Berry, J.J. Monitoring the stability of organometallic perovskite thin films. *J. Mater. Chem. A* **2015**, *3*, 21940–21945. [[CrossRef](#)]
15. Sharma, K.; Sharma, V.; Sharma, S.S. Dye-Sensitized Solar Cells: Fundamentals and Current Status. *Nanoscale Res. Lett.* **2018**, *13*, 381. [[CrossRef](#)] [[PubMed](#)]
16. Mesquita, I.; Andrade, L.; Mendes, A. Temperature Impact on Perovskite Solar Cells Under Operation. *ChemSusChem* **2019**, *12*, 2186. [[CrossRef](#)]
17. Torres, J.P.N.; Marques Lameirinhas, R.A.; Correia V. Bernardo, C.P.; Veiga, H.I.; dos Santos, P.M. A Discrete Electrical Model for Photovoltaic Solar Cells—d1MxP. *Energies* **2023**, *16*, 2018. [[CrossRef](#)]
18. Zhaoxu, S.; Kun, F.; Xiaofang, S.; Ying, L.; Wei, L.; Chuanzhong, X.; Gongyi, H.; Fei, Y. An Effective Method to Accurately Extract the Parameters of Single Diode Model of Solar Cells. *Nanomaterials* **2021**, *11*, 2615. [[CrossRef](#)]
19. Castro, R.; Silva, M. Experimental and Theoretical Validation of One Diode and Three Parameters-Based PV Models. *Energies* **2021**, *14*, 2140. [[CrossRef](#)]
20. Yuqiang, L.; Li, Y.; Wu, Y.; Yang, G.; Mazzarella, L.; Procel-Moya, P.; Tamboli, A.C.; Weber, K.; Boccard, M.; Isabella, O.; et al. High-Efficiency Silicon Heterojunction Solar Cells: Materials, Devices and Applications. *Mater. Sci. Eng. Rep.* **2020**, *147*, 100579.
21. Firoz K.; Singh, S.N.; Husain, M. Effect of illumination intensity on cell parameters of a silicon solar cell. *Sol. Energy Mater. Sol. Cells* **2010**, *94*, 1473–1476. [[CrossRef](#)]
22. Alves, T.; Torres, J.P.N.; Marques Lameirinhas, R.A.; Fernandes, C.A.F. Different Techniques to Mitigate Partial Shading in Photovoltaic Panels. *Energies* **2021**, *14*, 3863. [[CrossRef](#)]
23. Matsunaga, Y.; Oya, T. Development of Paint-Type Dye-Sensitized Solar Cell Using Carbon Nanotube Paint. *J. Nanotechnol.* **2019**, *2019*, 5081034. [[CrossRef](#)]

Disclaimer/Publisher’s Note: The statements, opinions and data contained in all publications are solely those of the individual author(s) and contributor(s) and not of MDPI and/or the editor(s). MDPI and/or the editor(s) disclaim responsibility for any injury to people or property resulting from any ideas, methods, instructions or products referred to in the content.